Scalable Computing: Practice and Experience, ISSN 1895-1767, http://www.scpe.org
© 2024 SCPE. Volume 25, Issues 3, pp. 2048–2061, DOI 10.12694/scpe.v25i3.2708

DETECTION METHOD OF TOURIST FLOW IN SCENIC SPOTS BASED ON KALMAN FILTER PREDICTION

XIAOYAN XU* AND LI ZHANG†

Abstract. The tourism industry has developed rapidly, but it is always limited by the environmental carrying capacity and cannot receive too many tourists at the same time. Therefore, it is very necessary to limit the number of tourists visiting at the same time based on traffic detection. To this end, the tourist scenic spot (TSS) traffic statistics system was designed. The system performed graying, binarization, image denoising, and morphological processing on the image. The pre-processed image used the background difference method based on mixed Gaussian background modeling to detect moving objects. The improved Hough transform circle detection method was used to identify the head target, and the Kalman filter (KF) was used to complete the target tracking. KF could predict the target trajectory accurately, and the improved Hough transform circle detection method could recognize the head under occlusion. The maximum missed detection rate of the statistical system was 3.2%, the minimum is 0, and the overall detection accuracy was the highest. The error rate of inbound passenger flow was 4.10%, and the error rate of outbound passenger flow was 3.0%. Using this system can control the tourist flow (TF) in the scenic spot and avoid safety accidents due to excessive passenger flow. And it is conducive to the sustainable development of the scenic spot.

Key words: Moving target detection; KF; Tourist flow in scenic spots; Hough transform circle detection

1. Introduction. In recent years, tourism has gradually become a leisure and lifestyle of people around the world. According to the figures released by the World Tourism Association, tourism ranked third in the global GDP growth in 2019. It is reported that the tourism industry (TI) has grown at a rate of 3.5%, far exceeding the growth rate of 2.5% of the world's GDP. Taking China as an example, TI provides nearly 80 million jobs, equivalent to 10.3% of the whole country. Meanwhile, the total output value of China's TI is about 10.9 trillion-yuan, accounting for 11.3% of China's economy. The rapid development of the global tourism market has led to the rapid development of China's domestic TI [1]. The TI of China has stepped into "mass tourism", and tourists' willingness to travel is increasing. It can be expected that TI will continue to thrive even in the post-epidemic period. However, due to the sharp increase in the number of tourists, the increase in tourist experience and traffic safety accidents of TSS has brought a great negative impact on TSS. Relevant departments have proposed measures to strengthen TF control to solve the hidden danger of urban traffic safety. As the carrying capacity of the urban population exceeds the carrying capacity, the tourist experience will be reduced. This has led to deterioration of the ecological environment and aggravation of environmental pollution, and it even triggers social security incidents [2-3]. If the TSS-TF can be accurately detected, it can prevent a large number of tourists from staying, achieve peak travel, improve the experience of TSS tourists, and promote the comprehensive development of TSS. In addition to tourism TSS, due to the development of the economy, various large transportation hubs and public places will be crowded, which will have a great impact on urban transportation and public places [4]. Therefore, if the passenger flow statistics are carried out for commercial locations, the operator can make reasonable decisions based on the changes in passenger flow, which leads to more benefits for the operator. The flow of visitors can be reflected in real-time through the statistics of passenger traffic at TSS and other cultural and entertainment venues. Thus, the development trend of tourism off-season and peak season is obtained, which is convenient to establish the corresponding safety warning mechanism. Real-time dispatching and management of passenger flow can be realized through the statistics of passenger flow at airports, subway stations and other transportation hubs. The passenger flow statistics of mobile vehicles such as buses and subways can be used for early warning management of overload.

*School of Tourism Management, Xinyang Agriculture and Forestry University, Xinyang, 464000, China
†School of Tourism Management, Xinyang Agriculture and Forestry University, Xinyang, 464000, China. Corresponding E-mail: li_zhang2023@outlook.com

Traditional TF detection mainly relies on empirical method, but it is difficult to meet the current demand due to its short time and low accuracy [5]. So how to detect TF faster and more accurately has become an important part of TSS management. This requires further deepening and improving the tourist experience, avoiding large-scale tourist detention, improving the quality of tourist service and ensuring the safety of tourists' lives and property. Therefore, the research will detect TF of tourism TSS by moving target detection method based on mixed Gaussian background modeling background difference method, Hough transform circle detection method, and KF moving target tracking method.

2. Related works. The research on monitoring methods of tourist TF in the industry has produced many research results. Rogowski M et al. proposed the MSTT tourist behavior monitoring system. The system used 39 pyroelectric sensors and survey data to obtain the space-time characteristics of TF. It realized the monitoring of mountaineering, automobile traffic, and the evaluation of illegal tourism. The system was feasible [6]. Kumaran N et al. proposed an abnormal behavior detection scheme in human group activities based on social behavior. The method included a feature description method using covariance matrix coding to realize optical flow expression and a covariance matrix model using mixed optical flow. This method could better simulate the group activities and identify the monitored abnormal events [7]. Lev et al. proposed a K-Means-based method to identify the spatial distribution characteristics of TSS TF. This method combined the location big data features to express the data source in a temporal and spatial manner, which analyzed the TF temporal features in combination with the distance measurement of dynamic time warping and K-Means. This method could analyze the flow time series type and identify the flow spatial distribution characteristics. The analysis results were helpful to the internal traffic and facility management of TSS [8]. Zimoch M et al. established a TF recognition system based on thermal map and SSD method. The system used edge image analysis, pre-trained SSD method, and displacement vector centroid algorithm combined with Siam network. In the Market 1501 data set, the system had a level 1 efficiency of 84.6% [9]. Du S et al. proposed a TSS tourist feature analysis method based on wavelet nonlinear transform. In spring and autumn, the TF changed greatly, while in winter it is relatively small. Inbound tourists showed obvious seasonal characteristics and showed clear characteristics of off-season and peak season [10].

Classic methods such as KF are often used in the industry to track human targets to improve the accuracy of TF detection. The research on KF has also produced many results. He L et al. combined adaptive KF with transient flow model and adaptive control to propose a real-time unsteady flow estimation method for multi-product pipelines. In this method, the linear flow field model combined with difference conversion and frequency response was used to replace the nonlinear flow model, which was applied to the linear compensation of the unsteady flow model. Under unpredictable conditions, this method could make the transient flow estimation error of linear model and conventional nonlinear model less than 0.5%, effectively overcoming the problems of traditional methods [11]. Zhang HF et al. proposed a detection method based on KF and wavelet transform for pitch target recognition. This method could well suppress the mixed white noise in the music. Compared with the fundamental frequency detection algorithm based on Fourier transform, its average recognition error rate in the full frequency range decreased by 0.89%, and its robustness was more ideal [12]. Yu X et al. applied the KF estimation model to cycle slip detection and repair. In this study, a cycle slip detection and repair method with strong adaptability was proposed, and then the KF estimation model was established by connecting the cycle slip detection equation and the state equation. KF estimation model could detect and repair all simulated cycle slips [13]. Yang J et al. adopted a new method based on differential KF to track the lag behavior of civil engineering structures. This method combined QR decomposition with strong tracking filtering to track the changes of structural parameters. The hysteresis curve obtained by the proposed algorithm was in good agreement with the test curve [14]. Zhou P et al. proposed a robust model-free adaptive predictive control method based on KF for quality control of molten iron in blast furnace. This control strategy could better overcome data loss, measurement noise and other problems [15].

To sum up, previous passenger flow statistics methods often use sensors and monitoring images to identify human targets. However, due to the complex situation of pedestrians entering side by side and people moving in both directions, these passenger flow statistics methods are not competent. Based on the complexity of TF motion, this research will propose a moving target detection method based on head tracking, which can improve the accuracy of moving human detection through real-time tracking of human head.

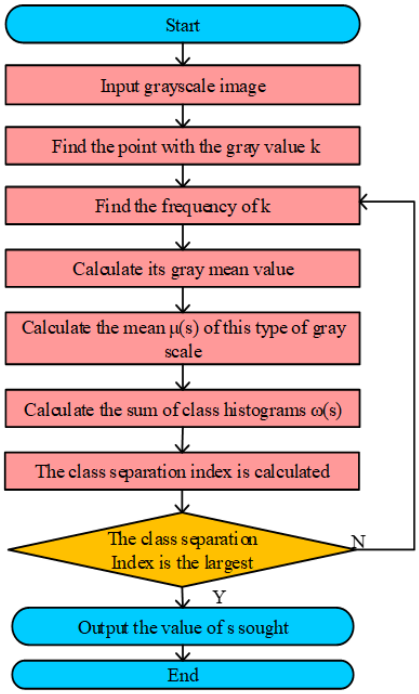

Fig. 3.1: The method of image graying

3. Tourism TSS-TF detection method based on KF prediction.

3.1. Video image preprocessing method.. In the passenger flow monitoring of TSS, the video image of TSS should be obtained first. When acquiring video images, the image has a certain degree of distortion due to the influence of various environmental factors such as noise, light and so on, so it must be preprocessed. The image preprocessing methods used in this study include image binarization, image graying, image denoising, and image morphology processing [16].

The method of image graying is to transform RGB three-channel image data of color image into single-channel image data for processing. The research uses the weighted average method to weighted average the RGB three components to obtain a more reasonable gray image. Image binarization is the process of changing the gray value of an image to make a color image into a black and white image. Its core is the selection of threshold. Otsu method is selected for threshold selection. The flow of Otsu algorithm is shown in Figure 3.1. First of all, it needs to find the point in the gray image with the gray value of k and find the frequency of the point. Then it needs to calculate its gray mean value, the sum of the gray mean value $\mu(s)$ and the class histogram $\omega(s)$ to calculate the class separation index. When the class separation index is maximum, the s value obtained is the best threshold of the image.

There are many methods for image denoising, among which median filtering can remove impulse noise and salt and pepper noise very well, and the edge of the image is not affected. Therefore, median filtering is used for denoising [17]. If the position of the pixel points to be processed in the image is (m, n), and the gray value of the point is shown in $g(m, n)$. Then the processing result of median filtering for the point is shown in formula (3.1).

$$g(m,n) = med\{f(m-v)(n-v), ..., f(m-1)(n-1), f(m,n), f(m+1)(n+1), ..., f(m+v)(n+v)\} \quad (3.1)$$

where $f(m, n)$ is the gray value at position (m, n), and $2v$ is the number of pixels in the filter window. Morphological processing refers to the use of a structural element in the image to perform a set operation on the original binary image to extract useful information of the image. The basic morphological operations include expansion,

corrosion, open, and close operations. The expansion process is that image a is expanded by structural element b, which is recorded as $a \oplus b$, where $\oplus$ is the expansion operator. Formula (3.2) is the expansion expression. w

$$a \oplus b = \{x \left| (\hat{b}_x \cap a) \neq \emptyset \right.\} \tag{3.2}$$

where x is the distance b first maps about the origin and then translates. Formula (3.3) is the expression of corrosion.

$$a \odot b = \{x \left| (\hat{b}_x \cap a) \neq \emptyset \right.\} \tag{3.3}$$

where $\odot$ is the operator of corrosion. Operation calculation is to corrode the binary image first and then expand it. The expression is shown in formula (3.4).

$$a \circ b = (a \circ b) \oplus b \tag{3.4}$$

where $\circ$ is the operator of the open operation. The close operation is to expand the binary image first and then corrode it. The expression is shown in formula (3.5).

$$a \bullet b = (a \oplus b) \odot b \tag{3.5}$$

where $\bullet$ is a closed operator. The above processing measures are conducive to extracting the required image information. It can reduce irrelevant information in video images, enhance useful information, and simplify image data, laying a foundation for subsequent target detection.

3.2. Moving target detection method based on background difference method of mixed Gaussian background modeling.. The pre-processed image is detected to recognize the moving human object in the image. Moving human detection is divided into two parts: moving target detection and pedestrian target recognition. Moving target detection is to detect the moving object in the sequence image, so as to obtain the region of the moving target. The commonly used moving target detection methods include optical flow method, inter-frame difference method, and background difference method. The optical flow method has many iterations and complex calculation, and it is generally difficult to realize real-time detection. The detection threshold of the inter-frame difference method is selected by manual experiments, and the adjustment steps are cumbersome [18]. So, the background difference method is selected.

The principle of background difference method is to subtract the current frame from the background image to get the difference value. The threshold is set in advance. If the difference value is greater than the set threshold, it is considered as a moving target. Otherwise, it is not a moving target. The algorithm expression is shown in formula (3.6) [19].

$$d(m,n) = \begin{cases} 0, |f_k(m,n) - b(m,n)| \leq t \\ 1, others \end{cases} \tag{3.6}$$

where $d(m,n)$ is the binary differential image, $f_k(m,n)$ represents the current frame image, $f_k(m,n)$ is the background image, and t is the threshold. The background difference method will change the image background in practical application, resulting in inaccurate target detection. Therefore, the background difference method generally needs to establish a background model to achieve real-time background update. In the monitoring area, most of the background images are modal. At this point, the background of each mode can be represented by a Gaussian function. Therefore, a variety of Gaussian models are used in the experiment to describe the background of multiple different modes. The gray value of the sequence image shall meet the Gaussian distribution of formula (3.7) below. w

$$p(x_t) = \sum_{i=1}^{k} w_{it}(x_t, g_{it}, \sum{}_{it}) \tag{3.7}$$

where, x_t is the pixel value at time t. w_{it}, g_{it}, and $\sum_{it}$ are the weight, mean, and covariance of the i-the Gaussian distribution at time t. The process of background difference method based on mixed Gaussian

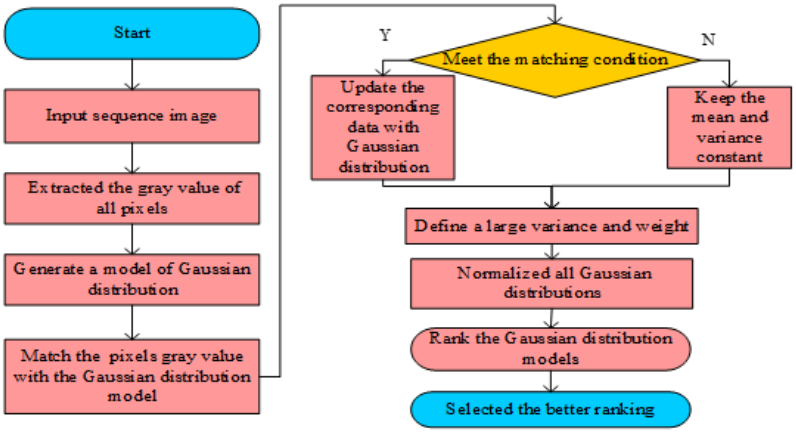

Fig. 3.2: Process of background difference method based on mixed Gaussian background modeling

background modeling is as follows: the sequence image needs to be input to extract the gray value of all pixels. Then the Gaussian distribution model is generated, and the gray value of the matching pixel is matched with the Gaussian distribution model. The update that meets the matching conditions corresponds to the data of the first Gaussian distribution. Otherwise, it needs to keep the mean and variance of the Gaussian distribution corresponding to the pixel unchanged, and then define a larger variance and weight. Then all the Gaussian distributions are normalized, and the Gaussian distribution models are sorted, and the better one is selected as the background model.

After the moving target in the sequence image is detected, the next step is to identify whether it is a pedestrian from the detected moving target. First of all, it needs to extract the edge of the detected binary image. Combining the scene of TF statistics, the Canny algorithm is selected for edge extraction. The Hough detection circle algorithm is used for head recognition in this study since the pedestrian head information in the monitoring area is approximately circular when the camera collects video images.

The main reason for choosing the Canny algorithm is its excellent edge detection performance, especially robustness in noisy environments [20-21]. The Canny algorithm reduces the effect of noise on edge detection by smoothing the image using a multi-stage algorithm. First, it smoothes the image using a Gaussian filter to filter out the noise. The potential edges are then found by calculating the gradient strength and direction of the image. Next, these edges are refined using non-maximal suppression (NMS) technique [22-23]. Finally, the Canny algorithm is able to effectively differentiate between true and false edges with the dual-thresholding algorithm and edge-connection technique. This series of fine-tuning steps gives the Canny algorithm a significant advantage in the accuracy of edge detection and the precision of edge localization. In this study, the clear and accurate head contour features extracted by the Canny algorithm lay a solid foundation for subsequent head recognition and target tracking, thus improving the overall system performance.

In the surveillance area, the head target can be effectively identified using the Hough transform when the camera captures the video image since the pedestrian head information usually presents an approximate circle. The core of the Hough transform lies in the parameter estimation, which realizes the double mapping from pixel coordinates to parameter space by converting the coordinate problem in the image into a point and line problem in the parametric coordinate system. However, it is more difficult to find complete circles in practical detections, so this study combines the geometrical properties of circles to make improvements. First, the radius threshold of head-like circles is set to exclude the maximum and minimum boundaries of the image. Second, all the points on each edge need to be searched. With these improvements, the Hough transform is able to exclude non-human targets from the moving targets recognized by the background difference method based on hybrid Gaussian background modelling, thus improving the accuracy of pedestrian recognition.

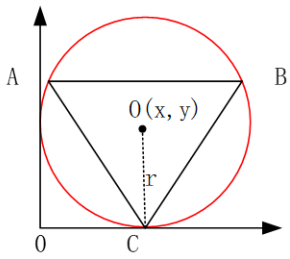

Fig. 3.3: Arc division diagram

When improving the Hough transform, it is necessary to use the idea of arc division to enhance the geometric features of incomplete circles to accurately calculate the coordinates of the centre of the circle and the radius. The structure diagram of arc division is shown in Figure 3.3. Firstly, the target boundary is equally divided into three arc segments AB, BC, and AC. This step is based on the geometrical properties of circles, and the maximum and minimum boundaries in the image are excluded by setting the radius threshold for head-like circles to ensure that a target close to the real head shape is detected. Next, all points on each arc segment need to be detected one by one to compute the centre coordinates and radius of the circle that can be determined through these three points. The advantage of the arc division method is that it can more accurately identify and label the circular target of a traveling human head by accurately calculating the features of each arc segment. This method can effectively identify the target even when the targets are partially overlapped, thus avoiding the detection omission due to the overlapping of images. This arc segmentation and computation method enables the detection algorithm to effectively exclude non-human targets in complex surveillance environments. It significantly improves the accuracy of pedestrian head recognition and provides reliable data support for subsequent target tracking and pedestrian traffic statistics.

3.3. Tracking method of head contour feature frame matching based on KF.. The background difference method based on mixed Gaussian background modeling can recognize the moving objects in the image. Canny algorithm and improved Hough detection circle algorithm can recognize the head objects and determine the detected moving objects as pedestrians [24-25]. The pedestrian is a moving target, so it is necessary to estimate and predict the direction of the moving target for tracking and matching.

In the research on pedestrian target tracking and matching, KF is selected as the core algorithm, mainly based on its excellent prediction and estimation capabilities. KF is a recursive algorithm that can effectively handle the state estimation problem of dynamic systems and is particularly well-suited to deal with noisy signal data. In pedestrian head contour feature matching tracking, KF can utilize the dynamic changes of pedestrian head contour features to provide accurate target state prediction through iterative calculations. In addition, KF does not need to save multiple previous input signals, so it takes up less memory and is very suitable for scenarios that require real-time processing of large amounts of data. Pedestrian targets can be effectively tracked and matched by using the edge detection results of pedestrian head contour features directly as the input of KF prediction, thereby improving the performance and efficiency of the entire system. The basic idea is to estimate the signal trend by recursion based on the characteristics and change rules of the dynamic signal itself. The algorithm has two steps: prior state prediction and observation correction. The equation of state is shown in formula (3.8) [26-27].

$$x_t = \alpha x_{t-1} + \beta s_{t-1} + z_{t-1} \tag{3.8}$$

where x_t is the state at time t. α and β are coefficients. s_{t-1} and $z_{t-1}$are the system control vector and process noise at $t-1$ time. Formula (3.9) is the observation equation. w

$$G_t = \delta x_t + v_t \tag{3.9}$$

where G_t is the observation variable at time t, G_t is the coefficient, and v_t is the observation noise. According to the state matrix and state estimation matrix of the current data, KF calculates the minimum mean square error

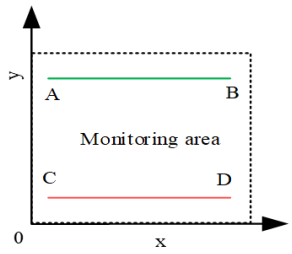

Fig. 3.4: Schematic diagram of tracking area division

matrix in the prediction matrix and corrects it. The minimum error after correction is the optimal prediction result. Formula (3.10) is the state prediction equation.

$$\hat{X}_t{}^- = \alpha \hat{X}_{t-1} + \beta s_{t-1} \tag{3.10}$$

where $\hat{X}_t{}^-$ is the optimal state prediction of the state variable. The covariance equation corresponding to the prediction matrix is shown in formula (3.11).

$$P_t{}^- = \alpha p_{t-1} \alpha_t^T + Q \tag{3.11}$$

where P_{t-1} is the $(t-1)*(t-1)$ covariance matrix, and p_{t-1} is the $p*p$-dimensional symmetric non-negative definite variance matrix. To make the prediction equation the best prediction result, the error gain can be minimized, and the error gain is formula (3.12).

$$K_t = P_t H^T R^{-1} \tag{3.12}$$

where H is the coefficient and R is the symmetric positive definite variance matrix. P_t is the covariance of the optimal estimate at the time of t as shown in formula (3.13). w

$$P_t = P_t{}^{-1} + HR^{-1}H^T? \tag{3.13}$$

The optimal estimation equation at the time of t is recorded as $\hat{X}_t$, and the calculation process of $\hat{X}_t$ is shown in formula (3.14).

$$\hat{X}_t = \hat{X}_t{}^- + K_t(z_t - H\hat{X}_t{}^-) \tag{3.14}$$

where K_t is the weight of the estimated value at the last time and the current measured value. KF prediction is also the inter-frame matching of head contour features. Its main function is data association, and then real-time update of target tracking chain. In the scope of photography, there are two most common conditions for pedestrians, one is ordinary access, the other is forward, backward, stop, and turn back. In these two cases, the state of the target tracking chain is: the establishment of the target tracking chain, the matching of the target tracking chain, the completion of the target tracking chain, and the disappearance of the target tracking chain. The monitoring area is divided into the tracking area as shown in Figure 3.4, and two entry and exit sign lines AB and BC are set. The positive direction of the y-axis is defined as in, and the negative direction is defined as out.

When a moving target chain passes AB sign line first and then BC sign line, the pedestrian is considered to enter. When the moving target chain passes through the BC marker line first and then AB marker line, it is considered as outflow. If there is a moving target chain entering and leaving from AB or BC, it is considered that the number of entry and exit remains unchanged. To sum up, the main flow chart of updating the target tracking chain is shown in Figure 3.5. After inputting the sequence image, it is necessary to recognize the head target, and then match the head with the pedestrian. The head feature contour data of the next frame is predicted by KF, and the target tracking chain is updated according to the optimal prediction result.

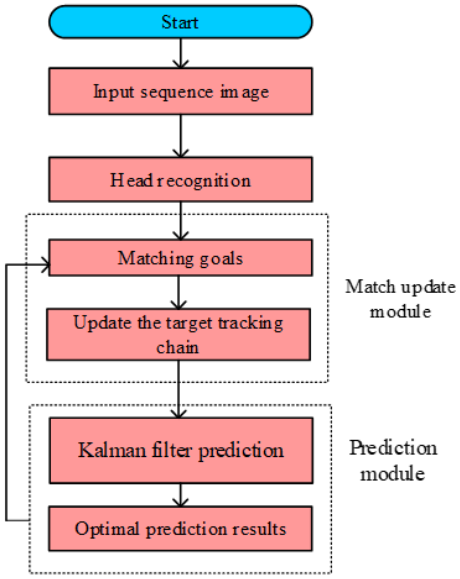

Fig. 3.5: Update moving target chain flowchart

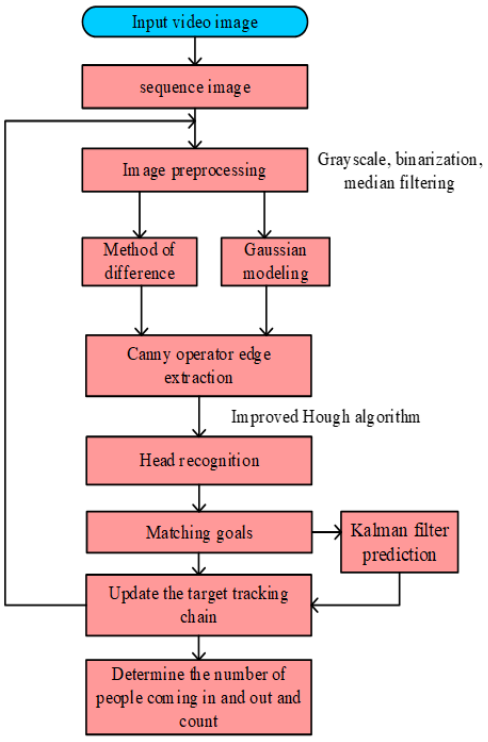

Fig. 3.6: Scenic spot human flow detection system framework

(a) Grayscale Image with Noise

(b) The filtered Grayscale Image

Fig. 4.1: Noise removal effect picture

The following passenger flow statistics system architecture is designed to realize the function of expected passenger flow statistics as shown in Figure 3.6. The architecture includes video image acquisition, and then it needs to be converted into sequence diagram and processed by graying, binarization, and median filtering. The processed image is recognized by the background difference method based on Gaussian modeling. Then the edge feature of the image is extracted by Canny operator, and the head is detected by improved Hough transform. Finally, KF is used to match pedestrian targets and count the number of people entering and exiting the monitoring sign line.

4. Analysis of application results of tourism TSS-TF detection system.. The fixed-focus camera HD720P USB is used for acquisition, and the image data is transmitted to the computer using the signal shielded wire. The image data are stored, processed and displayed by the computer. A high-performance computer is used as the core of the entire image signal analysis. The computer CPU is AMD Sempron (tm) Processor2800+Intel (R) Core (TM) i5-5200U CPU @ 2.20GHz2.2GHz, and the memory is 4G. After the completion of the hardware and software of the passenger flow statistics system, the actual measurement is carried out to check whether the system meets the system requirements. The test software environment is Visual Studio 2015 under Windows 7 operating system.

According to the application scenario, the relevant parameters of the passenger flow statistics system are adjusted and set according to the fixed angle of the camera and the height from the ground before the system runs. The TF at gate s1 and 2 of a TSS is counted in the experiment. The cameras of the No. 1 and No. 2 doors are fixed diagonally above the channel. The height of the installed camera from the ground is 3m, and the fitting radius of the system head is 18.3. Relevant scene videos need to be collected for statistics. In the process of statistics, each step of the system is processed separately, and the error causes are analyzed, and comparative experiments are carried out to verify the system performance. The comparison method is the micro-Doppler human motion detection method based on KF and convolution neural network (CNN) in [20] and the target detection algorithm based on improved Gaussian mixture model in [21].

The comparison of denoising effect between median filtering and other methods is shown in Figure 4.1. The median filter removes the noise of the original image well, the pedestrian target and background are more distinct. And the filtered image is clearer, which can help the subsequent system to better perform the target recognition task.

The result of target detection is shown in Figure 4.2. The images show that the edge detection results of this research method are more complete and clearer. The results of head target recognition are shown in the figure. Under the condition that pedestrian targets do not overlap, the improved Hough transform circle detection method in this study can completely recognize and mark the head circle of pedestrians. The contour feature extraction of pedestrians is also relatively complete. When the pedestrian head is partially overlapped,

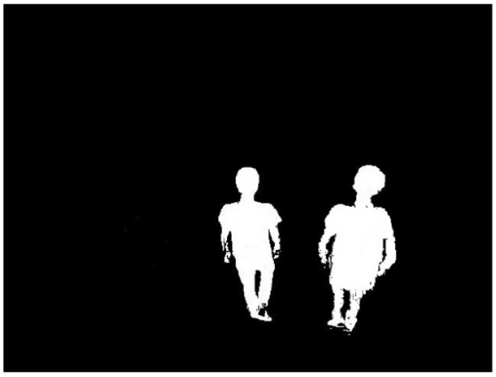

(a) Moving target detection diagram

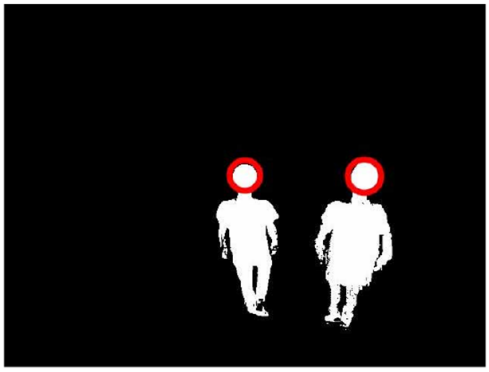

(b) Head target detection diagram without overlap

(c) Head target detection diagram in the case of partial overlap

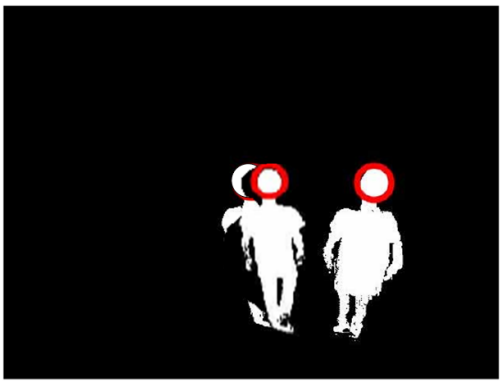

(d) Image of head target detection in most overlapping cases

Fig. 4.2: The result graph of target detection

the head target can also be recognized, which can avoid the problem of missing detection caused by the overlap of pedestrian images to a certain extent. However, when the pedestrian image completely overlaps or mostly overlaps, the method cannot recognize the head target because the overlapping part exceeds the recognition threshold.

Several frames of images are selected to be input into the KF device, and the pixel values of the center position x and y in the image are calculated. As time goes by, the predicted and actual values can be plotted. The x-coordinate trajectory and y-coordinate trajectory as shown in Figure 4.3 are obtained. In the prediction results of the head center coordinate predicted by KF, the error of the prediction of the center x coordinate is greater than that of the prediction of the y coordinate. When the number of pixel values is 5 and 7, the predicted value of x coordinate has a large deviation from the actual value. But in most cases, the prediction is more accurate. The predicted value of y coordinate has no big error all the time, which indicates that KF can better achieve the inter-frame matching of moving objects.

TF statistics at the entrance and exit of Gate 1 and Gate 2 from 12:00 to 16:00 are selected, and the statistical results are shown in Figure 4.4. The statistical results of gates 1 and 2 have missed inspection. However, the error between the TF statistical results of the system and the manual statistical results of gate 1 is slightly smaller than that of gate 2. This may be related to the different size of TF at the entrance and exit. The number of people in and out of gate 2 is far more than that of gate 1. In the case of large crowd density,

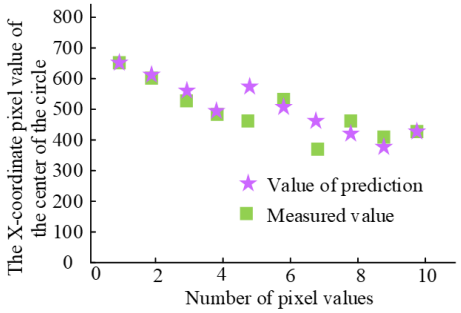

(a) Actual and predicted trajectories in X-coordinates of the center of the circle

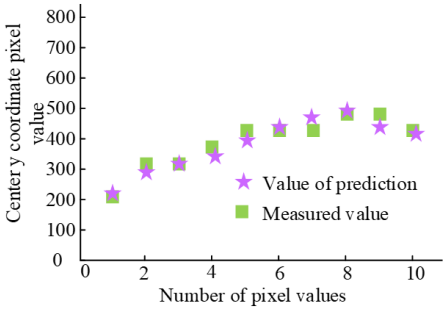

(b) Actual and predicted trajectories of Y-coordinates of the center of the circle

Fig. 4.3: KF center coordinates predicted trajectory

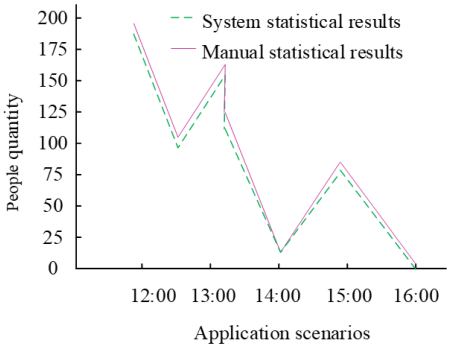

(a) Passenger flow statistics of Gate 1

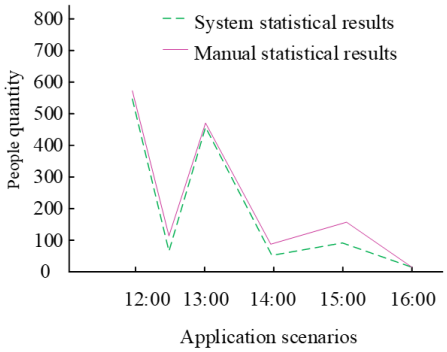

(b) Passenger flow statistics of Gate 2

Fig. 4.4: Statistical results of inbound and outbound traffic during 12:00 to 16:00

the problem of pedestrian head target occlusion is more serious. This is not conducive to the target recognition of the system, and the phenomenon of missing detection occurs from time to time.

The specific results of TF statistics of 9 sampled videos from two doorways are shown in Table 1. In this study, although the numbers of inflows and outflows are manually calculated, a number of measures are taken to minimize calculation errors to ensure the accuracy of the statistics. Firstly, each counting point is monitored by at least two specially trained observers who are responsible for recording the number of pedestrians passing through a particular entrance and exit. These observers use pre-designed counting equipment to minimize human error. Second, a video surveillance system is used in the study as a secondary validation tool to further validate the accuracy of the data. They can be corrected and validated against each other by comparing the manual counting data with the statistics automatically generated by the video analysis system. Finally, repeated measurements and cross-checks are performed on all data to ensure consistency and reliability. Overall, the error rate of the system's inbound passenger flow is 4.10%, and the error rate of the outbound passenger flow is 3.0%. The outflow statistics error of video number 9 is the largest, 0.3. The inflow statistics error of No. 8 video is the largest, 0.36. The statistical results of inflow and outflow of No. 1 video are both zero errors. The greater the number of people entering and leaving, the greater the statistical error.

Under different TF scales, the statistical results of this research system are compared with the micro-

Table 4.1: Sampling video traffic statistics result

Collect video number	The number of manual inflows is counted	Inflow system count	Inbound passenger flow error rate	The outflow volume is counted manually	System counts the outgoing volume	Error rate of outflow volume
1	22	22	0	5	5	0
2	55	54	0.035	10	10	0
3	111	110	0.036	35	34	0.027
4	80	78	0.005	5	5	0
5	126	120	0.032	6	6	0
6	320	324	0.031	31	30	0.096
7	680	660	0.028	240	236	0.029
8	519	500	0.036	330	319	0.085
9	841	820	0.034	1216	1200	0.03
Total	2760	2677	0.041	1216	1200	0.03

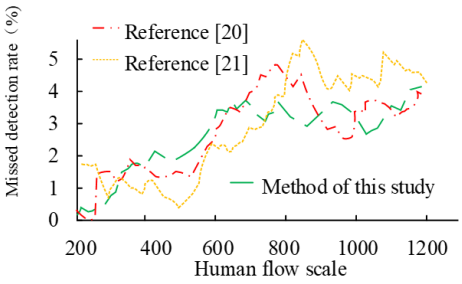

(a) Comparison of missed detection rates under different human flow scales

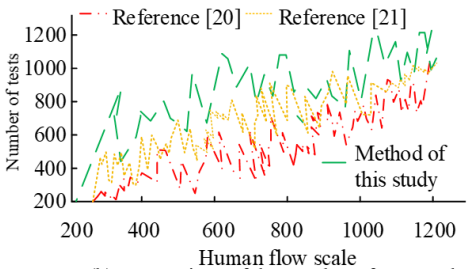

(b) Comparison of the number of tests under different human flow scales

Fig. 4.5: The statistical comparison results of the human flow of each method

Doppler human motion detection method based on KF and CNN and the target detection algorithm based on improved Gaussian mixture model, as shown in Figure 4.5. With the increase of TF, the number of missed inspections of each method gradually increases. However, the growth rate of the system in this study is slightly smaller than that of other methods, with a maximum miss rate of 4.0% and the minimum of 0. The rate of missed detection of other methods has risen rapidly. Its detection performance is relatively stable.

Single Shot MultiBox Detector (SSD), Mask Region-based Convolutional Neural Network (Mask R-CNN), and Multi-Scale Shared and Independent Feature Network (MSSIF-Net) were selected as the comparison algorithms to further prove that the proposed method in this study has better detection effect. The leakage rate, false detection rate, and accuracy rate of several algorithms are obtained as shown in Table 4.2. The leakage rate, false detection rate and accuracy rate of SSD were 5.96%, 6.11%, and 89.21%, respectively. The leakage rate, false detection rate and accuracy rate of Mask R-CNN were 3.87%, 3.95%, and 92.35%, respectively. The leakage rate, false detection rate and accuracy rate of MSSIF-Net were 2.30%, 2.57%, and 96.54%, respectively. The leakage rate, false detection rate and accuracy rate of the method proposed in the text were 1.25%, 1.34%, and 98.67%, respectively. In conclusion, the method proposed in the text has better detection effect.

5. Conclusions. The accurate prediction of the passenger flow of TSS can enable the relevant departments to efficiently reallocate various resources and public services, so as to organically integrate the resources in the region. For this reason, the TSS-TF statistical system was designed based on KF. The median filter had

Table 4.2: Detection performance of different algorithms

Methods	Leakage rate/%	Misdetection rate/%	Accuracy rate/%
SSD	5.96	6.11	89.21
Mask R-CNN	3.87	3.95	92.35
MSSIF-Net	2.30	2.57	96.54
Text methods	1.25	1.34	98.67

good denoising effect. The improved Hough transform circle detection method in this study could completely recognize and mark the head circle of the traveler without overlapping pedestrian targets. When the pedestrian's head overlapped partially but did not exceed the threshold, the head target could also be recognized. The total error rate of inbound passenger flow of TF statistical system was 4.10%, and the error rate of outbound passenger flow was 3.0%. With the increase of TF, the system in this study gradually raised, with the maximum missed detection rate of 3.2% and the minimum of 0. In the comparison method, the overall detection accuracy of the system was the highest. The system can be used to detect TSS-TF, help TSS control passenger flow, and promote the coordinated development of economic society and TI. However, in this study, human body recognition is based on head feature circle recognition. For objects with irregular shapes such as hair and hat, or objects with circles, the accuracy of human recognition will be reduced, thus affecting the accuracy of statistics. In future research, it is necessary to eliminate the interference of irregular object images.

Fundings. The research is supported by: Xinyang Agriculture and Forestry University Scientific Research Fund Project for Young Teachers (NO.20200214).

REFERENCES

[1] Hcia, E. The role of tourism in the development of the city. *Transportation Research Procedia*. **39** pp. 104-111 (2019)
[2] Aly, S. & Gutub, A. Intelligent recognition system for identifying items and pilgrims. *NED University Journal Of Research*. **15**, 17-23 (2018)
[3] Kim, S., Guy, S., Hillesland, K. & Others Velocity-based modeling of physical interactions in dense crowds. *The Visual Computer*. **31** pp. 541-555 (2015)
[4] Aly, S., AlGhamdi, T., Salim, M. & Others Information gathering schemes for collaborative sensor devices. *Procedia Computer Science*. **32** pp. 1141-1146 (2014)
[5] Sridevi, N. & Meenakshi, M. Efficient reconfigurable architecture for moving object detection with motion compensation. *Indonesian Journal Of Electrical Engineering And Computer Science*. **23**, 802-810 (2021)
[6] Rogowski, M. Monitoring System of tourist traffic (MSTT) for tourists monitoring in mid-mountain national park, SW Poland. *Journal Of Mountain Science*. **17**, 2035-2047 (2020)
[7] Kumaran, N. & Reddy, U. Classification of human activity detection based on an intelligent regression model in video sequences. *IET Image Processing*. **15**, 65-76 (2020)
[8] Lv Q. G, W., Yu, Q., Spatial, L. & Characteristics, T. Identification of scenic flow based on Location Big Data. *Information Technology*. **2022**, 93-97 (0)
[9] Zimoch, M. & Markowska-Kaczmar, U. Human flow recognition using deep networks and vision methods. *Engineering Applications Of Artificial Intelligence*. **104**, 1-10434 (2021)
[10] Du, S., Bahaddad, A., Jin, M. & Model, Z. - A CASE OF ZHANGJIAJIE. *Fractals: An Interdisciplinary Journal On The Complex Geometry Of Nature*. **2022**, 1-22401 (0)
[11] He, L., Gong, J., Wen, K., Wu, C. & Min, Y. New Method Based on Model-Free Adaptive Control Theory and Kalman Filter for Multi-Product Unsteady Flow State Estimation. *Journal Of Energy Resources Technology*. **143**, 2-10 (2021)
[12] Zhang H. F, Z. Fundamental Frequency Wavelet Autocorrelation Detection Method Based on Kalman Filter. *Electronic Design Engineering*. **30**, 77-81 (2022)
[13] Yu, X. & Xia, S. highly adaptable method for GNSS cycle slip detection and repair based on Kalman filter. *Survey Review*. **53** pp. 169-182 (2020)
[14] Yang, J., Xia, Y., Yan, Y., Yan, Y., Sun, L. & Sun, L. Modified Strong Tracking System Identification Method Based on Square Root Center Difference Kalman Filter for Civil Structures. *International Journal Of Structural Stability And Dynamics*. **21**, 1354-1361 (2021)
[15] Zhou, P., Zhang, S., Wen, L., Fu, J. & Wang, H. Kalman Filter-Based Data-Driven Robust Model-Free Adaptive Predictive Control of a Complicated Industrial Process. *IEEE Transactions On Automation Science And Engineering*. **19**, 788-803 (2021)
[16] Zhu, H., Yan, X., Tang H. , Y. & Yuan, F. Moving object detection with Deep CNNs. *IEEE Access*. **8** pp. 29729-29741 (2020)

[17] Kaysi, I., Alshalalfah, B., Shalaby, A. & Others Users' evaluation of rail systems in mass events: case study in Mecca, Saudi Arabia. *Transportation Research Record*. **2350**, 111-118 (2013)
[18] And, M. and collection algorithms for collaborative sensor devices using dynamic cluster heads. *Trends In Applied Sciences Research*. **8**, 55-72 (2013)
[19] Singh, A., Satapathy, S., Roy, A. & Others Ai-based mobile edge computing for iot: Applications, challenges, and future scope. *Arabian Journal For Science And Engineering*. pp. 1-31 (2022)
[20] Saeed, T., Mutashar, S., Abed, A., Mahmuod, H. & Abd-Elghany, S. Human Motion Detection through Wall Based on Micro-Doppler Using Kalman Filter Combined with Convolutional Neural Network. *International Journal Of Intelligent Engineering And Systems*. **12**, 317-327 (2019)
[21] Su, Y. Target detection algorithm and data model optimization based on improved Gaussian mixture model. *Microprocessors And Microsystems*. **81**, 1-10379 (2021)
[22] Roy, P., Saumya, S., Singh, J. & Others Analysis of community question-answering issues via machine learning and deep learning: State-of-the-art review. *CAAI Transactions On Intelligence Technology*. **8**, 95-117 (2023)
[23] Alharthi, N. & Gutub, A. Data visualization to explore improving decision-making within Hajj services. *Scientific Modelling And Research*. **2**, 9-18 (2017)
[24] Curtis, S., Zafar, B., Gutub, A. & Others Right of way: Asymmetric agent interactions in crowds. *The Visual Computer*. **29** pp. 1277-1292 (2013)
[25] Abdelgawad, H., Shalaby, A., Abdulhai, B. & Others Microscopic modeling of large-scale pedestrian-vehicle conflicts in the city of Madinah, Saudi Arabia. *Journal Of Advanced Transportation*. **48**, 507-525 (2014)
[26] Sufi, F., Alsulami, M. & Gutub, A. Automating global threat-maps generation via advancements of news sensors and AI. *Arabian Journal For Science And Engineering*. **48**, 2455-2472 (2023)
[27] Singh, A., Gutub, A., Nayyar, A. & Others Redefining food safety traceability system through blockchain: findings, challenges and open issues. *Multimedia Tools And Applications*. **82**, 21243-21277 (2023)

Edited by: Zhengyi Chai
Special issue on: Data-Driven Optimization Algorithms for Sustainable and Smart City
Received: Oct 18, 2023
Accepted: Mar 1, 2024